European Review for Medical and Pharmacological Sciences 2020; 24: 6486-6493

MiR-204 inhibits inflammation and cell apoptosis in retinopathy rats with diabetic retinopathy by regulating Bcl-2 and SIRT1 expressions

F. QI[1], X. JIANG[2], T. TONG[2], H. CHANG[2], R.-X. LI[1,2]

[1]Department of Ophthalmology, Liaoning University of Traditional Chinese Medicine, Shenyang, China
[2]Department of Ophthalmology, the 4th People's Hospital of Shenyang, Shenyang, China

Abstract. – OBJECTIVE: To explore the influences of micro ribonucleic acid (miR)-204 on the rats with diabetic retinopathy by regulating the expressions of B-cell lymphoma 2 (Bcl-2) and sirtuin 1 (SIRT1).

MATERIALS AND METHODS: A total of 36 Sprague-Dawley rats were randomly assigned into normal group (n=12), model group (n=12), and miR-204 mimics group (n=12). No treatment was performed in the normal group, the diabetic retinopathy model was established in model group, and miR-204 mimics were administered for intervention after modeling in the inhibitor group. After 7 d, materials were sampled for detection. The expressions of Bcl-2 and SIRT1 were detected via immunohistochemistry, and their relative protein expression levels were determined via Western blotting (WB). Quantitative Polymerase Chain Reaction (qPCR) was performed to detect the expression of miR-204, and the content of inflammatory factors interleukin (IL)-6, IL-18, and tumor necrosis factor-α (TNF-α) was measured using enzyme-linked immunosorbent assay (ELISA). Finally, cell apoptosis was evaluated via terminal deoxynucleotidyl transferase-mediated dUTP nick end labeling (TUNEL).

RESULTS: Immunohistochemistry results showed that the positive expression levels of Bcl-2 and SIRT1 were substantially lower in the model and miR-204 mimics groups than those in the normal group ($p<0.05$), and their positive expression levels in miR-204 mimics group were notably higher than those in model group ($p<0.05$). According to Western blot (WB) results, the relative protein expression levels of Bcl-2 and SIRT1 markedly declined in the other two groups compared with those in the normal group ($p<0.05$), while miR-204 mimics group exhibited remarkably higher relative protein expression levels of Bcl-2 and SIRT1 than the model group ($p<0.05$). The results of qPCR revealed that the relative expression level of miR-204 was markedly lowered in model and miR-204 mimics groups compared with that in the normal group ($p<0.05$), and its relative expression level in miR-204 mimics group was remarkably higher than that in the model group. It was found through enzyme-linked immunosorbent assay (ELISA) that compared with normal group, the other two groups had substantially increased content of IL-6, IL-18, and TNF-α ($p<0.05$), and the content of IL-6, IL-18, and TNF-α in miR-204 mimics group was markedly lower than that in the model group ($p<0.05$). According to TUNEL results, the apoptosis rate of cells rose substantially in the other two groups compared with that in the normal group ($p<0.05$), while was notably lower in the miR-204 mimics group than that in the model group ($p<0.05$).

CONCLUSIONS: MiR-204 up-regulates Bcl-2 and SIRT1 expressions to inhibit the inflammation and cell apoptosis in rats with diabetic retinopathy.

Key Words:
Diabetic retinopathy, MiR-204, Inflammation, Apoptosis.

Introduction

Diabetic retinopathy is one of the most common blinding diseases in the clinical ophthalmology, whose incidence rate is on the rise with the increasing number of diabetic patients. Persistent high blood glucose-induced damage to small vessels can cause lesions of the retinas in diabetic patients, thereby inducing diabetic retinopathy[1,2]. Diabetic retinopathy mainly leads to damage to the visions of patients and blindness in severe cases, causing the loss of labor ability in patients[3,4]. Therefore, it is of great urgency to delve into the related pathogenesis and pathological reactions of diabetic retinopathy.

Corresponding Author: Ruoxi Li, MD; e-mail: sysylrx@126.com

With the development of the research on diabetic retinopathy, it has been realized by researchers that the pathological reactions of diabetic retinopathy are a series of complex cascade reactions, in which inflammation and cell apoptosis play important roles, further aggravating damage. Studies[5,6] have found that B-cell lymphoma 2 (Bcl-2), with an anti-apoptosis effect, and sirtuin 1 (SIRT1), with an anti-inflammation effect, can protect against retinal cell damage well, so they are considered as the potential action targets for the improvement of diabetic retinopathy.

Micro ribonucleic acid (miR)-204, an important non-coding RNA, has a vital regulatory effect on several downstream cellular signaling pathways, thereby modulating the development and progression of multiple diseases[7,8]. The present study, therefore, aims to explore the influences of miR-204 on rats with diabetic retinopathy by regulating Bcl-2 and SIRT1 expressions.

Materials and Methods

Laboratory Animals

A total of 36 specific pathogen-free laboratory Sprague-Dawley (SD) rats aged 1 month old [Shanghai SLAC Laboratory Animal Co., Ltd., certificate No.: SCXK (Shanghai, China) 2014-0003)] were fed with normal diet and sterile filtered water daily in the Experimental Animal Center in a 12/12 h light-dark cycle and at normal room temperature and humidity. This study was approved by the Animal Ethics Committee of Liaoning University of Traditional Chinese Medicine Animal Center.

Experimental Reagents and Instruments

Streptozotocin (Sigma-Aldrich, St. Louis, MO, USA), miR-204 mimics (MCE, Monmouth Junction, NJ, USA), primary antibodies: anti-Bcl-2 antibody, and anti-SIRT1 antibody and secondary antibodies (Abcam, Cambridge, MA, USA), terminal deoxynucleotidyl transferase-mediated dUTP nick end labeling (TUNEL) apoptosis assay and enzyme-linked immunosorbent assay (ELISA) kits, AceQ quantitative polymerase chain reaction (qPCR) SYBR Green Master Mix kit and HiScript II Q RT SuperMix for qPCR [+genomic deoxyribonucleic acid (+gDNA) wiper] kit (Vazyme Biotech, Nanjing, China), optical microscope (Leica DMI 4000B/DFC425C, Wetzlar, Germany), and fluorescence quantitative PCR instrument (ABI 7500, Applied Biosystems, Foster City, CA, USA).

Animal Grouping and Treatment

Thirty-six SD rats were divided into normal group (n=12), model group (n=12), and inhibitor group using a random number table, and they were adaptively fed in the Experimental Animal Center for 7 d for subsequent experiments.

The rats in the normal group were normally fed, without any treatment. After the model of diabetic retinopathy was prepared, the rats in the model group were normally raised, without any intervention, while those in the miR-204 mimics group were intraperitoneally injected with miR-204 mimics daily at a dose of 50 μL/100 g. At 7 d after modeling, all the rats were sacrificed for sampling.

Establishment of Diabetic Retinopathy Models

First, the prepared 1% streptozotocin solution was intraperitoneally injected into rats at a dose of 60 mg/kg, and 3 d later, venous blood was drawn from the tails of the rats to detect blood glucose. The blood glucose >16.7 mmol/L indicates successful modeling.

Sampling

After successful anesthesia, the retinal tissues of 6 rats in each group were directly taken, rinsed with normal saline, and stored in Eppendorf (EP; Hamburg, Germany) tubes at -80°C for later Western blotting (WB) and qPCR. The remaining 6 rats in each group were fixed through perfusion for sampling as follows: the thoracic cavity of the rats was cut open to expose the heart and perfused with 400 mL of 4% paraformaldehyde through the left atrial appendage. Then, the retinal tissues were taken out, soaked and fixed in 4% paraformaldehyde for immunohistochemistry detection and TUNEL assay.

Immunohistochemistry

The pre-paraffin-embedded tissues were first sliced into 5 μm-thick sections, extended in warm water at 42°C, mounted, and baked. Then, the paraffin-embedded tissue sections were soaked successively in xylene solution and gradient ethanol for routine deparaffinization and hydration. Subsequently, the resulting sections were immersed in citrate buffer and heated for 3 min and braised for 3 times (5 min/time) in a micro-wave oven for complete antigen retrieval. After rinsing, the tissue sections were added dropwise with endogenous peroxidase blocker, reacted for 10 min, rinsed, and sealed using goat serum in drops for

20 min. After the goat serum blocking solution was removed, the tissue sections were incubated with the anti-Bcl-2 and SIRT1 primary antibodies (1:200) in a refrigerator at 4°C overnight. On the next day, the rinsed sections were incubated again with the secondary antibody solution for 10 min and fully rinsed. Afterwards, the sections were reacted with streptomycin avidin-peroxidase solution for 10 min and added dropwise with diaminobenzidine (DAB) for color development, and the cell nuclei were counter-stained with hematoxylin. Finally, the sections were sealed and observed.

Western Blotting

The cryopreserved retinal tissues were added with lysis buffer, bathed on ice for 1 h, and centrifuged at 14,000 g in a centrifuge for 10 min. Subsequently, the proteins were quantified by the bicinchoninic acid (BCA) method (Pierce, Rockford, IL, USA), and the concentration of proteins in the tissues was calculated based on the absorbance measured using a microplate reader and the standard curve. Afterwards, the proteins were denaturalized and isolated from the tissue specimens *via* sodium dodecyl sulphate-polyacrylamide gel electrophoresis (SDS-PAGE) until it was observed that the marker protein was at the bottom of the glass plate in a straight line, and the resulting proteins were transferred onto a polyvinylidene difluoride (PVDF) membrane (Roche, Basel, Switzerland), sealed with the blocking buffer for 1.5 h, and incubated successively with anti-Bcl-2 and anti-SIRT1 primary antibodies (1:1,000) and secondary antibodies (1:1,000). After rinsing, the proteins were reacted with chemiluminescent reagent for 1 min for complete image development in the dark.

QPCR

Total RNAs were first extracted from tissue specimens and reversely transcribed into cDNAs using the reverse transcription kit in a 20 μL reaction system as follows: reaction at 51°C for 2 min, pre-denaturation at 96°C for 10 min, denaturation at 96°C for 10 s, and annealing at 60°C for 30 s, for 40 cycles. Finally, the relative expression levels of the related mRNAs were calculated with GAPDH as an internal reference. The specific primer sequences are shown in Table I.

TUNEL Assay

The tissues embedded in paraffin earlier were made into 5 μm-thick sections, extended in warm water at 42°C, mounted, and baked. Then, these sections were routinely de-paraffinized and hydrated successively with xylene solution and gradient ethanol. Subsequently, the resulting sections were added dropwise with TdT reaction solution and reacted in the dark for 1 h. Then, the reaction was terminated through incubation with deionized water in drops for 15 min. After the activity of endogenous peroxidase was blocked by hydrogen peroxide, the sections were added dropwise with working solution. Following reaction for 1 h, the sections were rinsed, added with DAB solution in drops for color development, and rinsed again. Finally, they were sealed and observed.

ELISA

The fresh retinal tissues were ground to be minced. Then, according to the instructions of the ELISA kit, the samples and standards were separately loaded, and added with biotinylated antibody working solution and enzyme-conjugated substance working solution, and the plate was washed. Finally, the products were measured at 450 nm in a microplate reader.

Statistical Analysis

In this study, Statistical Product and Service Solutions (SPSS) 20.0 software (IBM Corp., Armonk, NY, USA) was employed for statistical analysis, and enumeration data were expressed as mean ± standard deviation. The data conforming to normal distribution and homogeneity of variance were subjected to *t*-test. Comparison be-

Table I. List of primer sequences.

Gene	Primer sequence
MiR-204	Forward: 5' TCCACTTCCAAGCTGAGCGAG 3' Reverse: 5' GTCCAGGGCATGATGGTTCT 3'
GAPDH	Forward: 5' ACGGCAAGTTCAACGGCAGTGGCA 3' Reverse: 5' GAAGACGCCAGTAGACTCCACGAC 3'
U6	Forward: 5' GCGCGTCGTGAAGCGTTC 3' Reverse: 5' GTGCAGGGTCCGAGGT 3'

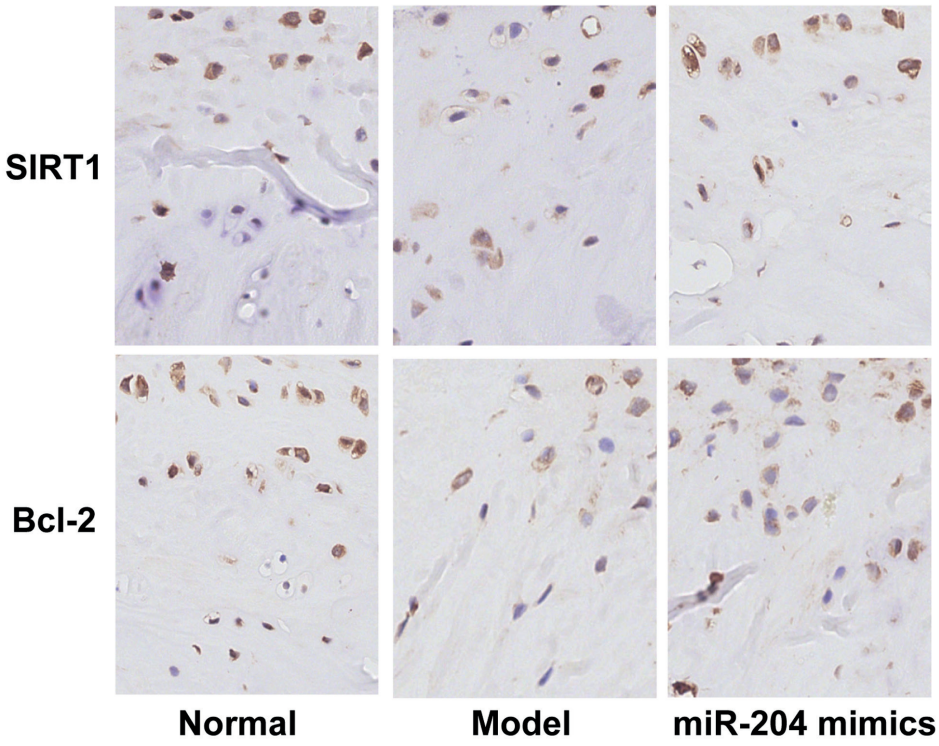

Figure 1. Expressions of Bcl-2 and SIRT1 detected *via* immunohistochemistry (magnification: 200×).

tween multiple groups was done using One-way ANOVA test followed by post-hoc test (Least Significant Difference). $p<0.05$ indicated statistically significant differences.

Results

Immunohistochemistry Results

As shown in Figure 1, tan represents positive expression, and the positive expressions of Bcl-2 and SIRT1 were increased in normal group and decreased in the other two groups. According to the statistical results (Figure 2), compared with that in normal group, the average optical density of tissues with positive expressions of Bcl-2 and SIRT1 was substantially raised in the other two groups, showing statistically significant differences ($p<0.05$), and the average optical density in miR-204 mimics group was notably higher than that in the model group, with statistically significant differences ($p<0.05$).

WB Results

The Bcl-2 and SIRT1 proteins were higher in normal group, but lower in the other two groups (Figure 3). The statistical results revealed that the relative protein expression levels of Bcl-2 and SIRT1 in the model and miR-204 mimics groups were markedly lower than those in the normal group, with statistically significant differences

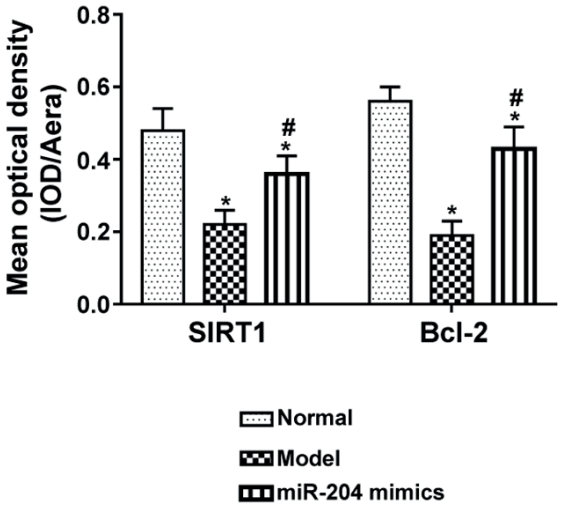

Figure 2. Positive expressions of SIRT1 and Bcl-2 in each group. Note: $^{*}p<0.05$ *vs.* normal group, and $^{\#}p<0.05$ *vs.* model group.

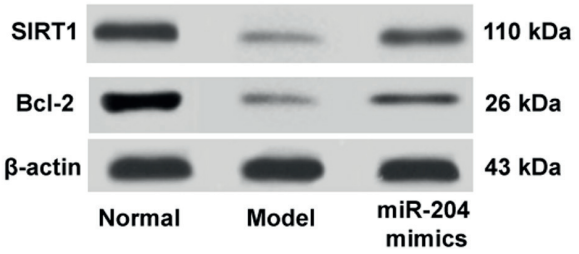

Figure 3. Expressions of related proteins detected *via* WB.

(p<0.05), while they were remarkably higher in miR-204 mimics group than those in the model group, showing statistically significant differences (p<0.05) (Figure 4).

QPCR Results

In comparison with that in the normal group, the relative expression level of miR-204 was decreased markedly in the other two groups, with a statistically significant difference (p<0.05), and its relative expression level in miR-204 mimics group was remarkably higher than that in the model group, showing a statistically significant difference (p<0.05) (Figure 5).

ELISA Results

As shown in Figure 6, the content of interleukin (IL)-6, IL-18, and TNF-α rose substantially in the other two groups compared with that in the normal group, showing a statistically significant difference (p<0.05), while it was markedly lower in miR-204 mimics group than that in the model group, with a statistically significant difference (p<0.05).

Cell Apoptosis Detected Via TUNEL

Apoptotic cells showed the tan color, and it was found that normal group had fewer apoptotic cells than the other two groups (Figure 7). Compared with normal group, the other two groups exhibited a substantial increase in the average optical density of TUNEL-positive apoptotic cells, showing a statistically significant difference (p<0.05), while their average optical density in miR-204 mimics group was notably lower than that in the model group, with a statistically significant difference (p<0.05) (Figure 8).

Discussion

Diabetic retinopathy, a major complication of diabetes, causes severe and even irreversible damage to the vision of patients, which remains one of the leading causes of blindness in patients. Particularly, as the social development and improvement of peoples' living standard, diabetic retinopathy has become increasingly more prevalent, with the rise in the morbidity rate of diabetes. Ultimately, most diabetic patients lose labor capacity due to blindness[9,10]. Both cell apoptosis and inflammation play an important role in the pathogenesis of diabetic retinopathy. Further studies[11-13] have demonstrated that after long-term high blood glucose-induced injuries and patho-

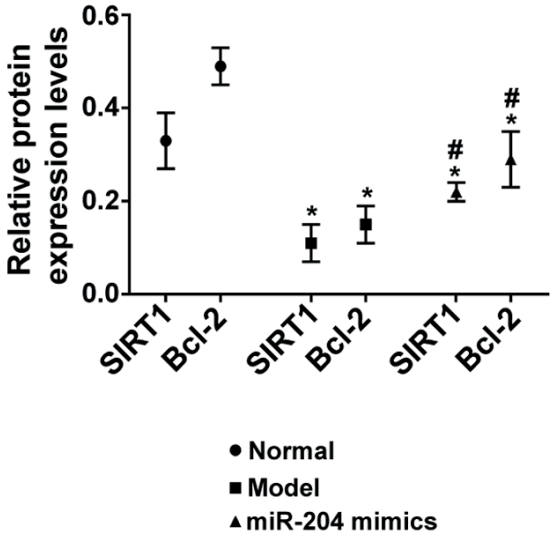

Figure 4. Relative protein expression levels in each group. Note: $^{*}p$<0.05 *vs.* normal group, and $^{\#}p$<0.05 *vs.* model group.

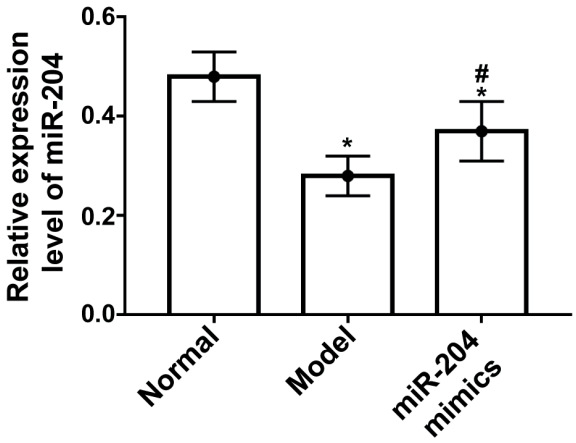

Figure 5. Relative expression level of miR-204 in each group. Note: $^{*}p$<0.05 *vs.* normal group, and $^{\#}p$<0.05 *vs.* model group.

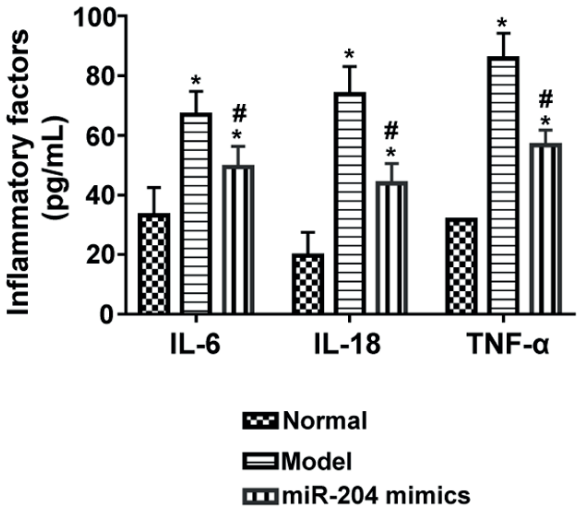

Figure 6. Content of inflammatory factors in each group. Note: $^{*}p<0.05$ *vs.* normal group, and $^{\#}p<0.05$ *vs.* model group.

genic changes in small vessels of retinas, inflammatory responses will occur in the retinas under the action of injurious factors, and the content of massive inflammatory factors, such as IL-6, IL-18, and TNF-α will be aberrantly raised. Besides, the infiltration of large numbers of inflammatory factors at persistently high concentrations can further activate apoptosis-associated pathways, resulting in the apoptosis of massive retinal cells. Therefore, inhibiting inflammation and cell apoptosis is extremely vital for diabetic retinopathy. Persistent high-level inflammation and cell apoptosis can also induce the tissue fibrosis. In other words, they can promote the proliferation of fibroblasts, and induce fibrosis of tissues ultimately, which is not conducive to the repair and treatment of diabetic retinopathy[14,15]. Bcl-2, as an important player in the apoptosis-associated pathways, maintains apoptosis balance, and it has an anti-apoptosis effect and can resist the pro-apoptosis effect of Bax in apoptosis well. Additionally, SIRT1, an NAD-dependent histone deacetylase, exerts a vital anti-apoptosis effect by participating in anti-inflammatory responses. According to some researches[16,17], SIRT1 can inhibit inflammatory responses and oxidative stress after injury, thereby protecting retinal cells from apoptosis. The results of this study revealed that Bcl-2 and SIRT1 were abnormally lowly expressed in the retinal tissues of diabetic retinopathy model rats and notably lower than those in normal rats, suggesting that the declines in the anti-inflammation and anti-apoptosis abilities of the retinal tissues in diabetic retinopathy model rats result in high degrees of inflammation and cell apoptosis.

MiR-204, a non-coding RNA, is currently considered to play critical regulatory roles in organisms, which has been confirmed to bear close relationships with the onset of multiple diseases. Zeng et al[18] and Lee et al[19] have demonstrated that miR-204 degrades or suppresses the downstream mRNAs *via* pairing with the corresponding untranslated regions in the downstream target genes, thereby regulating transcription and modulating such pathological processes as cell proliferation, differentiation, and apoptosis. Zheng et al[20] discovered that, miR-204 is closely associated with the development and progression of multiple diseases, and it can also exert important effects and influences on numerous pathological reactions in diseases by regulating numerous cellular signaling pathways, so it is recognized as an important regulator in diseases. The novelty of this study was mainly that we first explored the role of miR-204 in a rat model of diabetic retinopathy and tried to study its molecular mechanism. In our investigation, it was found that the expression level

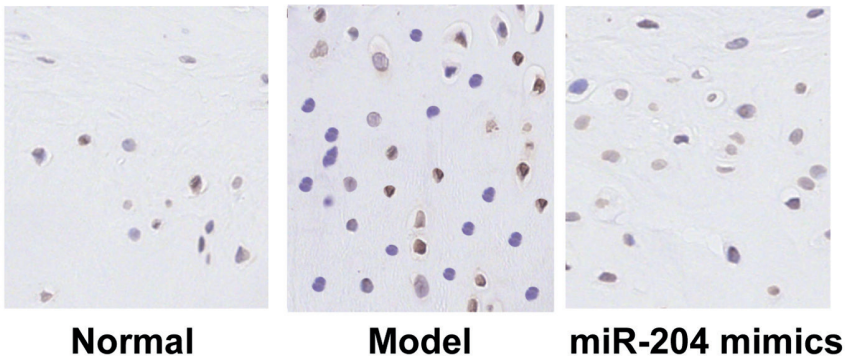

Figure 7. Cell apoptosis in each group (magnification: 200×).

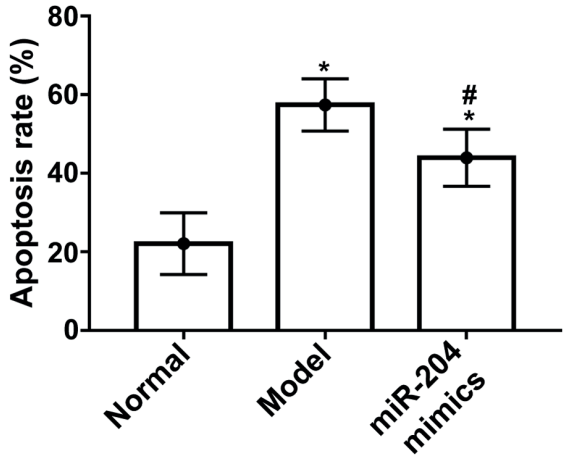

Figure 8. Cell apoptosis rate in all groups. Note: $^{*}p<0.05$ *vs.* normal group, and $^{\#}p<0.05$ *vs.* model group.

of miR-204 was substantially lower in the retinal tissues in the diabetic retinopathy model rats than that in normal rats, implying that miR-204 is abnormally expressed in the retinal tissues of the diabetic retinopathy model rats and involved in the onset of diabetic retinopathy. Moreover, miR-204 mimics substantially increased the relative expression level of miR-204, further promoting the high expressions of Bcl-2 and SIRT1 and decreasing the content of inflammatory factors IL-6, IL-18, and TNF-α. Thus, it can be concluded that miR-204 inhibits the inflammation and cell apoptosis in rats with diabetic retinopathy by upregulating Bcl-2 and SIRT1 expressions.

Conclusions

Briefly, miR-204 upregulates Bcl-2 and SIRT1 expressions to inhibit the inflammation and cell apoptosis in rats with diabetic retinopathy.

Conflict of Interest

The Authors declare that they have no conflict of interests.

References

1) Ding J, Wong TY. Current epidemiology of diabetic retinopathy and diabetic macular edema. Curr Diab Rep 2012; 12: 346-354.
2) Gouliopoulos NS, Kalogeropoulos C, Lavaris A, Rouvas A, Asproudis I, Garmpi A, Damaskos C, Garmpis N, Kostakis A, Moschos MM. Association of serum inflammatory markers and diabetic retinopathy: a review of literature. Eur Rev Med Pharmacol Sci 2018; 22: 7113-7128.
3) Ting DS, Cheung GC, Wong TY. Diabetic retinopathy: global prevalence, major risk factors, screening practices and public health challenges: a review. Clin Exp Ophthalmol 2016; 44: 260-277.
4) Stitt AW, Curtis TM, Chen M, Medina RJ, McKay GJ, Jenkins A, Gardiner TA, Lyons TJ, Hammes HP, Simo R, Lois N. The progress in understanding and treatment of diabetic retinopathy. Prog Retin Eye Res 2016; 51: 156-186.
5) Li L, Yuan L, Luo J, Gao J, Guo J, Xie X. MiR-34a inhibits proliferation and migration of breast cancer through down-regulation of Bcl-2 and SIRT1. Clin Exp Med 2013; 13: 109-117.
6) Takayama K, Ishida K, Matsushita T, Fujita N, Hayashi S, Sasaki K, Tei K, Kubo S, Matsumoto T, Fujioka H, Kurosaka M, Kuroda R. SIRT1 regulation of apoptosis of human chondrocytes. Arthritis Rheum 2009; 60: 2731-2740.
7) Mikhaylova O, Stratton Y, Hall D, Kellner E, Ehmer B, Drew AF, Gallo CA, Plas DR, Biesiada J, Meller J, Czyzyk-Krzeska MF. VHL-regulated MiR-204 suppresses tumor growth through inhibition of LC3B-mediated autophagy in renal clear cell carcinoma. Cancer Cell 2012; 21: 532-546.
8) Lee Y, Yang X, Huang Y, Fan H, Zhang Q, Wu Y, Li J, Hasina R, Cheng C, Lingen MW, Gerstein MB, Weichselbaum RR, Xing HR, Lussier YA. Network modeling identifies molecular functions targeted by miR-204 to suppress head and neck tumor metastasis. PLoS Comput Biol 2010; 6: e1000730.
9) Gulshan V, Peng L, Coram M, Stumpe MC, Wu D, Narayanaswamy A, Venugopalan S, Widner K, Madams T, Cuadros J, Kim R, Raman R, Nelson PC, Mega JL, Webster DR. Development and validation of a deep learning algorithm for detection of diabetic retinopathy in retinal fundus photographs. JAMA 2016; 316: 2402-2410.
10) Freiberg FJ, Pfau M, Wons J, Wirth MA, Becker MD, Michels S. Optical coherence tomography angiography of the foveal avascular zone in diabetic retinopathy. Graefes Arch Clin Exp Ophthalmol 2016; 254: 1051-1058.
11) Tang J, Du Y, Lee CA, Talahalli R, Eells JT, Kern TS. Low-intensity far-red light inhibits early lesions that contribute to diabetic retinopathy: in vivo and in vitro. Invest Ophthalmol Vis Sci 2013; 54: 3681-3690.
12) Li J, Wang JJ, Yu Q, Wang M, Zhang SX. Endoplasmic reticulum stress is implicated in retinal inflammation and diabetic retinopathy. FEBS Lett 2009; 583: 1521-1527.
13) Joussen AM, Poulaki V, Le ML, Koizumi K, Esser C, Janicki H, Schraermeyer U, Kociok N, Fauser S, Kirchhof B, Kern TS, Adamis AP. A central role for inflammation in the pathogenesis of diabetic retinopathy. FASEB J 2004; 18: 1450-1452.
14) Kilari S, Yang B, Sharma A, McCall DL, Misra S. Increased transforming growth factor beta (TGF-β) and pSMAD3 signaling in a murine model for

contrast induced kidney injury. Sci Rep 2018; 8: 6630.

15) van der Velden JL, Wagner DE, Lahue KG, Abdalla ST, Lam YW, Weiss DJ, Janssen-Heininger YMW. TGF-β1-induced deposition of provisional extracellular matrix by tracheal basal cells promotes epithelial-to-mesenchymal transition in a c-Jun NH2-terminal kinase-1-dependent manner. Am J Physiol Lung Cell Mol Physiol 2018; 314: L984-L997.

16) Zhao S, Li T, Li J, Lu Q, Han C, Wang N, Qiu Q, Cao H, Xu X, Chen H, Zheng Z. MiR-23b-3p induces the cellular metabolic memory of high glucose in diabetic retinopathy through a SIRT1-dependent signalling pathway. Diabetologia 2016; 59: 644-654.

17) Mortuza R, Feng B, Chakrabarti S. MiR-195 regulates SIRT1-mediated changes in diabetic retinopathy. Diabetologia 2014; 57: 1037-1046.

18) Zeng Y, Yi R, Cullen BR. Recognition and cleavage of primary microRNA precursors by the nuclear processing enzyme Drosha. EMBO J 2005; 24: 138-148.

19) Lee Y, Ahn C, Han J, Choi H, Kim J, Yim J, Lee J, Provost P, Radmark O, Kim S, Kim VN. The nuclear RNase III Drosha initiates microRNA processing. Nature 2003; 425: 415-419.

20) Zheng P, Chen L, Yuan X, Luo Q, Liu Y, Xie G, Ma Y, Shen L. Exosomal transfer of tumor-associated macrophage-derived miR-21 confers cisplatin resistance in gastric cancer cells. J Exp Clin Cancer Res 2017; 36: 53..